Bloch oscillations and Wannier-Stark localization in a tight-binding lattice with increasing intersite coupling

S. Longhi*

Dipartimento di Fisica and Istituto di Fotonica e Nanotecnologie del CNR, Politecnico di Milano, Piazza L. da Vinci 32, I-20133 Milano, Italy

(Received 2 June 2009; published 22 July 2009)

The onset of Bloch oscillations in an exactly solvable one-dimensional tight-binding lattice model with increasing hopping rates between adjacent sites is theoretically investigated. In particular, it is shown that Wannier-Stark localization is attained at a finite value of the applied dc field. An optical realization of the lattice model, based on light transport in engineered waveguide arrays, is also proposed.

DOI: 10.1103/PhysRevB.80.033106 PACS number(s): 72.10.Bg, 42.82.Et, 42.25.Fx, 03.75.Lm

Bloch oscillations (BOs), i.e., the oscillatory motion of electrons in a periodic periodical induced by a dc field, are one of the most striking predictions of the semiclassical theory of electronic transport.[1] In ordinary crystals these oscillations cannot be observed because collisions dephase the coherent motion of electrons on a time scale, which is much shorter than the BO period $T_B=h/(e\mathcal{E}a)$, where a is the lattice period, e is the electronic charge, and $\mathcal{E}$ is the applied dc electric field. In solid-state physics, BOs have been observed after the advent of high-quality semiconductor superlattices,[2] culminating in the observation of terahertz radiation from coherently oscillating electrons.[3,4] More recently, the analogs of electronic BOs have been predicted and experimentally observed for ultracold atoms[5] and Bose-Einstein condensates[6] in tilted optical lattices, for optical waves in arrays of evanescently coupled optical waveguides[7] and photonic superlattices,[8] and for sound waves in acoustical superlattices.[9] In the simplest single-band and tight-binding one-dimensional lattice model, the existence of BO is basically related to the circumstance that the energy spectrum changes from continuous (a band structure with delocalized Bloch eigenstates) in absence of the external field to a discrete ladder energy spectrum and localized eigenfunctions (Wannier-Stark states) when the external field is applied.[10] It is remarkable that the transition from extended (Bloch) to localized (Wannier-Stark) states occurs, in principle, for any infinitesimally small dc electric field. Recently, the onset of BOs in several lattice model generalizations has been theoretically investigated, including BOs in nonlinear lattices,[11] BOs in aperiodic lattices with long-range-correlated disorder,[12] BOs with spatially inhomogeneous dc fields,[13] BOs in quasicrystals,[14] BOs for interacting bosons,[15] and BOs in disordered lattices with interparticle interaction.[16] In particular, it was shown that BOs survive in aperiodic lattices with long-range disorder, providing a useful tool to measure the energy width of the delocalized phase states.[12] As most of previous works have focused on lattice models with some disorder or nonlinearity, BOs in ordered lattices with inhomogeneous hopping rates have not received much attention yet.

In this Brief Report the existence and properties of BOs in a one-dimensional tight-binding lattice model with inhomogeneous intersite coupling is theoretically investigated. A noteworthy feature of this model is to be exactly solvable and to exhibit a threshold dc field for Wannier-Stark localization. An optical realization of the lattice model, based on light transport in circularly curved waveguide arrays, is also proposed.

We consider a tight-binding Hamiltonian with an external dc electric field on a one-dimensional lattice of spacing a

$$\mathcal{H}=-\sum_{n=1}^{\infty}J_n(|n\rangle\langle n+1|+|n+1\rangle\langle n|)-e\mathcal{E}a\sum_{n=1}^{\infty}n|n\rangle\langle n|, \quad (1)$$

where $|n\rangle$ is a Wannier state localized at site n and $\mathcal{E}$ is the external uniform dc electric field. The intersite coupling is restricted to nearest neighbors and the hopping rate J_n between sites n and $(n+1)$ is assumed to linearly increase with site index n according to $J_n=\sigma n$ with $\sigma>0$. The energy of Wannier state $|n\rangle$ is taken to be independent of site n and is thus removed from Eq. (1). A possible realization of the tight-binding Hamiltonian (1) will be discussed below. In terms of the Wannier amplitudes $c_n(t)=\langle n|\Psi(t)\rangle$, the Schrödinger equation with $\hbar=1$ reads

$$i\frac{dc_n}{dt}=-J_nc_{n+1}-J_{n-1}c_{n-1}-Fnc_n, \quad (2)$$

where we have set $F=ea\mathcal{E}$ and assumed $c_n=0$ for $n\leq 0$. Alternatively, one can use a representation in terms of Bloch waves $|\kappa\rangle\equiv[a/(2\pi)]^{1/2}\Sigma_n\exp(in\kappa a)|n\rangle$ with $-\pi/a\leq\kappa<\pi/a$ (see, for instance, Ref. 17). In the latter representation, it can be readily shown that the evolution equation for the Bloch amplitude $S(\kappa,t)\equiv\langle\kappa|\Psi(t)\rangle=[a/(2\pi)]^{1/2}\Sigma_nc_n(t)\exp(-in\kappa a)$ reads

$$i\frac{\partial S}{\partial t}=-\frac{i}{a}[F+2\sigma\cos(\kappa a)]\frac{\partial S}{\partial\kappa}+\sigma\exp(i\kappa a)S, \quad (3)$$

where we used the relation $J_n=n\sigma$. In order to determine the energy spectrum E of Hamiltonian (1), it is convenient to work in the Bloch representation. We then search for a solution to Eq. (3) in the form $S(\kappa,t)=G(\kappa)\exp(-iEt)$. The function $G(\kappa)$ can be formally written as $G(\kappa)=G(-\pi/a)\exp[ia\varphi(\kappa)]$, where we have set

$$\varphi(\kappa) = \int_{-\pi/a}^{\kappa} dq \frac{E - \sigma \exp(iqa)}{F + 2\sigma \cos(qa)}. \quad (4)$$

Note that any eigenvector Ψ of energy E for Hamiltonian (1) that corresponds to a localized state, i.e., for which $\Sigma_n |c_n|^2 < \infty$, admits of a Bloch representation with regular (i.e., with no singularities) amplitude $G(\kappa)$ satisfying the periodic boundary condition $G(\pi/a) = G(-\pi/a)$.[18] An inspection of the integral on the right-hand side of Eq. (4) indicates that the amplitude G is singular for $\sigma \geq F/2$, whereas it is regular in the opposite case. We may therefore conclude that all the eigenstates of Hamiltonian (1) are extended for $0 \leq F < 2\sigma$ and localized for $F > 2\sigma$, a localization-delocalization transition occurring at the critical value $F = F_c = 2\sigma$. Moreover, for $F > 2\sigma$ the periodicity condition $\varphi(\pi/a) = 2l\pi/a$ ($l = 0, \pm 1, \pm 2, \pm 3, \ldots$) for the Bloch amplitude G shows that Hamiltonian (1) has a discrete Wannier-Stark energy spectrum given by

$$E_l = E_0 + \frac{2\pi l}{T_B}, \quad l = 0, \pm 1, \pm 2, \ldots, \quad (5)$$

where we have set

$$T_B \equiv \int_{-\pi}^{\pi} \frac{d\xi}{F + 2\sigma \cos \xi} = \frac{2\pi}{\sqrt{F^2 - 4\sigma^2}} \quad (6)$$

and

$$E_0 \equiv \frac{\sigma}{T_B} \int_{-\pi}^{\pi} \frac{d\xi \cos \xi}{F + 2\sigma \cos \xi} = \frac{1}{2}(\sqrt{F^2 - 4\sigma^2} - F). \quad (7)$$

As the energy levels are equally spaced, BOs of period T_B are thus found for Hamiltonian (1) when the external forcing F is above the critical value $F_c = 2\sigma$. Note that the BO period is corrected, as compared to the usual value $2\pi/F$ in a tight-binding homogeneous lattice, by the rate σ of the coupling increase between adjacent lattice sites according to Eq. (6). In particular, the BO period diverges near the localization-delocalization transition point $F = F_c$. To obtain a semiclassical description of BOs for a wave packet in the lattice model (1), it is worth observing that the solution $c_n(t)$ to the discrete Eq. (2) in the Wannier representation can be obtained from that of the continuous problem $i\partial\psi/\partial t = \mathcal{H}_e\psi$ with effective Hamiltonian $\mathcal{H}_e = -\sigma x \exp(ip) - \sigma(x-1)\exp(-ip) - Fx$ after setting $c_n(t) = \psi(x=n,t)$, where $p = -i\partial_x$ is the momentum operator in the continuous problem. The evolution equations for mean values of wave-packet position $\langle x \rangle$ and momentum $\langle p \rangle$ are then obtained from the Ehrenfest theorem using the effective Hamiltonian $\mathcal{H}_e$, i.e., $id\langle x \rangle/dt = \langle [x, \mathcal{H}_e] \rangle$ and $id\langle p \rangle/dt = \langle [p, \mathcal{H}_e] \rangle$. After computation of the commutators and taking the semiclassical limit, the resulting equations read explicitly

$$\frac{d}{dt}\langle x \rangle \simeq 2\sigma \langle x \rangle \sin\langle p \rangle, \quad \frac{d}{dt}\langle p \rangle \simeq F + 2\sigma \cos\langle p \rangle. \quad (8)$$

The condition $F > F_c = 2\sigma$ for the existence of BOs is retrieved from the semiclassical Eq. (8) after observing that for $0 \leq F < 2\sigma$ the momentum $\langle p \rangle$ reaches asymptotically a steady-state value, given by $\pi - \arccos[F/(2\sigma)]$, and hence the mean position $\langle x \rangle$ is exponentially growing at asymptotic times. As an example, Figs. 1(a) and 1(b) show the evolution of an initial Gaussian wave packet for an external force F below [Fig. 1(a)] and above [Fig. 1(b)] the critical value F_c, as obtained by numerical integration of Eq. (2). In the figures, the path $\langle x \rangle$ of the wave packet as predicted by the semiclassical Eq. (8) is also shown as a dotted line. Note that in the BO regime, the period of BO turns out to be in excellent agreement with the value T_B predicted by Eq. (6). Figures 1(c) and 1(d) show the evolution of site occupation amplitudes $|c_n|$ for the same conditions of Figs. 1(a) and 1(b) but for single site excitation at initial time. Note that the breathing mode, associated with BOs in the regime $F > F_c$, is strongly asymmetric and the wave-packet center of mass is not at rest as in the usual breathing oscillatory modes of BOs in a lattice with uniform hopping rates (see, for instance, Ref. 17). The asymmetry of the breathing oscillations simply arises because of the gradient in the hopping rate, which facilitates the particle hopping toward the direction of increasing coupling.

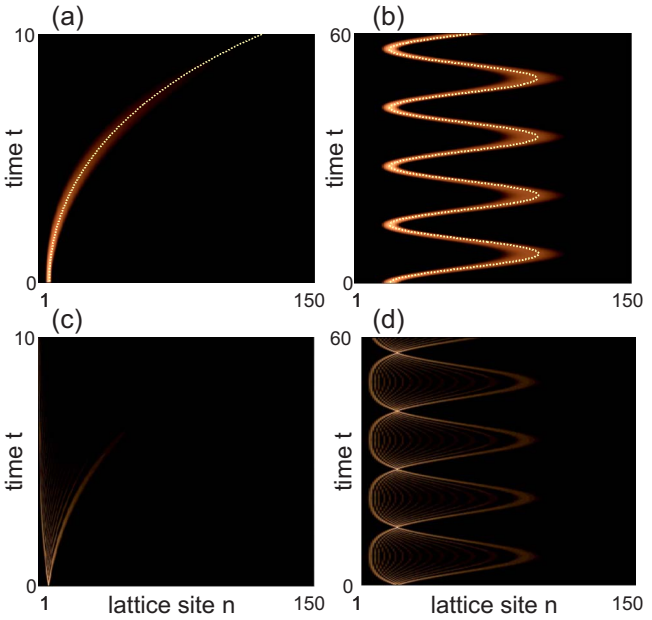

FIG. 1. (Color online) Evolution of amplitudes $|c_n(t)|$ for the tight-binding lattice model (1) for an input Gaussian wave packet $c_n(0) = \exp[-(n-20)^2/16]$ in (a) and (b), and for single-site excitation $c_n(0) = \delta_{n,20}$ in (c) and (d). Parameter values are $F = 0.35$ and $\sigma = 0.2$ in (a) and (c), $F = 0.6$ and $\sigma = = 0.2$ in (b) and (d). The dotted curves in (a) and (b) are the wave-packet center-of-mass trajectories as predicted by the semiclassical analysis [Eq. (8)].

An experimentally accessible realization of the lattice model (1) is provided by light transport in a chain of equal circularly curved evanescently coupled channel optical waveguides in the geometrical arrangement schematically shown in Fig. 2(a). Arrays of coupled waveguides have been successfully used in the past few years as an accessible laboratory tool to visualize in space the classical analogs of BOs (Ref. 7) and other coherent quantum phenomena encountered in atomic, molecular, or solid-state physics.[19] In particular, the current technological advances in waveguide fabrication enable a precise control of geometrical and material param-

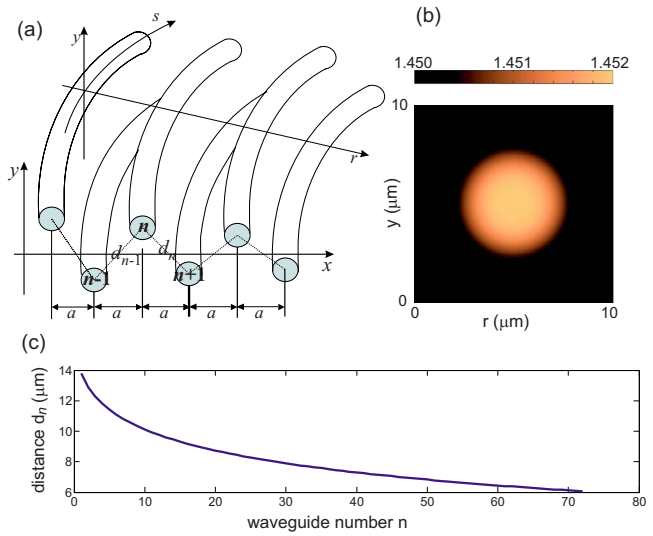

FIG. 2. (Color online) (a) Schematic of a chain of optical waveguides that realizes the lattice model (1). (b) Refractive index profile of the circular channel waveguides used in the simulations. (c) Distance d_n between adjacent waveguides n and $(n+1)$ in the chain that realizes a linear increase in the hopping rate J_n.

eters so as to engineer coupling rates in a prescribed way with accuracy (see, for instance, Ref. 20). Indicating by $c_n(s)$ the modal field amplitude of light waves at wavelength λ trapped in the nth waveguide of the chain, in the tight-binding and nearest-neighbor approximations light transport in the chain is described by a set of coupled-mode equations analogous to Eq. (2), where time t is replaced by the curvilinear spatial coordinate s, measured along the curved axis of the $n=0$ waveguide, J_n is the coupling rate between waveguides n and $(n+1)$, $F=2\pi n_s a/(R\lambda)$, where a is the (uniform) spacing between adjacent waveguides along the x axis, n_s is the substrate refractive index, and R is the radius of curvature of the circularly curved waveguides.[19] Coupled-mode equations can be derived from the scalar and paraxial Schrödinger-type wave equation that describes propagation of the electric field envelope ψ in the waveguide reference frame (r,y,s) [see Fig. 2(a)],[19,21]

$$i\lambda\frac{\partial\psi}{\partial z}=-\frac{\lambda^2}{2n_s}\left(\frac{\partial^2}{\partial r^2}+\frac{\partial^2}{\partial y^2}\right)\psi+V(r,y)\psi-\frac{n_s r}{R}\psi, \qquad (9)$$

where $V(r,y)\simeq n_s-n(r,y)$ and $n(r,y)$ is the s-invariant refractive index profile of the waveguide chain. The coupling rate J_n can be controlled by varying the distance d_n between adjacent waveguides n and $(n+1)$. For circularly curved waveguides and in a wide distance range, J_n is generally very well described by the exponential law $J_n=A\exp(-\gamma d_n)$, where the parameters A and γ depend on waveguide geometry and refractive index change.[22] A linear increase in the coupling rate $J_n=\sigma n$ can be thus obtained by properly decreasing the distances d_n of adjacent waveguides in the chain as the site number n increases. We checked the validity of the tight-binding lattice approximation for the waveguide chain of Fig. 2(a) and the occurrence of BOs by direct numerical

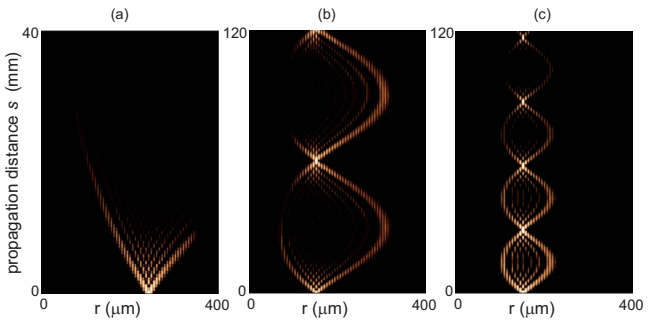

FIG. 3. (Color online) Evolution of integrated beam intensity in the (r,s) plane for single waveguide excitation of the circularly curved chain of Fig. 2(a) and for decreasing values of the radius of curvature (a) $R=2.3$ m, (b) $R=0.8$ m, and (c) $R=0.4$ m. Other parameter values are given in the text.

simulations of Eq. (9) using standard pseudospectral methods. The refractive index profile of each waveguide used in numerical simulations is shown in Fig. 2(b) and corresponds to a circular super-Gaussian shape with maximum index change $\Delta n=0.002$. At the wavelength $\lambda=633$ nm (red), the numerically computed coupling rate $J(d)$ between two waveguides placed at a distance d turns out to be fitted, with excellent accuracy, by the relation $J(d)=A\exp(-\gamma d)$ with $A\simeq 24.6$ mm^{-1} and $\gamma\simeq 0.466$ μm^{-1}. The array comprises a total number $N=73$ of waveguides, equally spaced along the x axis by the distance $a=6$ μm [see Fig. 2(a)]. In the simulations, we assumed coupling rate gradient $\sigma=0.02$ mm^{-1}, which is attained by assuming for the distance d_n between adjacent waveguides n and $(n+1)$ in the chain the behavior shown in Fig. 2(c). It should be noted that at low-index sites $(1\leq n\leq\sim 6)$, couplings among non-nearest-neighbor waveguides are not negligible; however, in our simulations excitation of such boundary waveguides is small and long-range coupling effects turn out to be negligible over the considered propagation distances. The strength of force $F=2\pi n_s a/(R\lambda)$ is changed by varying the bending radius of curvature R. In particular, the critical value $F_c=2\sigma$ for Wannier-Stark localization corresponds to a radius of curvature $R_c\simeq 2.159$ m. As an example, Figs. 3(a)–3(c) show the numerically computed evolution of integrated beam intensity $\int dy|\psi(r,y,s)|^2$ in the (r,s) plane for single-site excitation at the input plane[23] and for decreasing values of the radius of curvature R. Note that as the bending radius changes from below [Fig. 3(a)] to above [Figs. 3(b) and 3(c)] of the Wannier-Stark localization, a localized breathing mode is clearly observed with a BO cycle [$T_B\simeq 62$ mm in Fig. 3(b) and $T_B\simeq 29.6$ mm in Fig. 3(c)], which turns out to be in excellent agreement with the theoretical value predicted by Eq. (6).

In conclusion, the onset of BOs in an exactly solvable one-dimensional tight-binding lattice model, with inhomogeneous hopping rates and showing Wannier-Stark localization at a critical dc field, has been theoretically investigated. An optical realization of the lattice model, based on light propagation in engineered waveguide arrays, has been also proposed.

*longhi@fisi.polimi.it

[1] F. Bloch, Z. Phys. **52**, 555 (1928); C. Zener, Proc. R. Soc., London **A145**, 523 (1934).
[2] L. Esaki and R. Tsu, IBM J. Res. Dev. **14**, 61 (1970).
[3] C. Waschke, H. G. Roskos, R. Schwedler, K. Leo, H. Kurz, and K. Köhler, Phys. Rev. Lett. **70**, 3319 (1993).
[4] K. Leo, Semicond. Sci. Technol. **13**, 249 (1998).
[5] M. Ben Dahan, E. Peik, J. Reichel, Y. Castin, and C. Salomon, Phys. Rev. Lett. **76**, 4508 (1996); S. R. Wilkinson, C. F. Bharucha, K. W. Madison, Q. Niu, and M. G. Raizen, *ibid.* **76**, 4512 (1996).
[6] B. P. Anderson and M. A. Kasevich, Science **282**, 1686 (1998).
[7] R. Morandotti, U. Peschel, J. S. Aitchison, H. S. Eisenberg, and Y. Silberberg, Phys. Rev. Lett. **83**, 4756 (1999); T. Pertsch, P. Dannberg, W. Elflein, A. Bräuer, and F. Lederer, *ibid.* **83**, 4752 (1999); H. Trompeter, T. Pertsch, F. Lederer, D. Michaelis, U. Streppel, A. Bräuer, and U. Peschel, *ibid.* **96**, 023901 (2006); N. Chiodo, G. Della Valle, R. Osellame, S. Longhi, G. Cerullo, R. Ramponi, P. Laporta, and U. Morgner, Opt. Lett. **31**, 1651 (2006); H. Trompeter, W. Krolikowski, D. N. Neshev, A. S. Desyatnikov, A. A. Sukhorukov, Yu. S. Kivshar, T. Pertsch, U. Peschel, and F. Lederer, Phys. Rev. Lett. **96**, 053903 (2006).
[8] R. Sapienza, P. Costantino, D. Wiersma, M. Ghulinyan, C. J. Oton, and L. Pavesi, Phys. Rev. Lett. **91**, 263902 (2003); V. Agarwal, J. A. del Rio, G. Malpuech, M. Zamfirescu, A. Kavokin, D. Coquillat, D. Scalbert, M. Vladimirova, and B. Gil, *ibid.* **92**, 097401 (2004).
[9] H. Sanchis-Alepuz, Y. A. Kosevich, and J. Sanchez-Dehesa, Phys. Rev. Lett. **98**, 134301 (2007); Z. He, S. Peng, F. Cai, M. Ke, and Z. Liu, Phys. Rev. E **76**, 056605 (2007).
[10] Beyond the single-band approximation, Wannier-Stark states are actually resonances because of Zener tunneling ZT and BOs are thus damped, see, for instance, M. Gluck, A. R. Kolovsky, and H. J. Korsch, Phys. Rep. **366**, 103 (2002). However, in this work we assume that ZT is negligible.
[11] D. Cai, A. R. Bishop, N. Grønbech-Jensen, and M. Salerno, Phys. Rev. Lett. **74**, 1186 (1995).
[12] F. Dominguez-Adame, V. A. Malyshev, F. A. B. F. de Moura, and M. L. Lyra, Phys. Rev. Lett. **91**, 197402 (2003); E. Diaz, F. Dominguez-Adame, Yu. A. Kosevich, and V. A. Malyshev, Phys. Rev. B **73**, 174210 (2006); F. A. B. F. de Moura, L. P. Viana, M. L. Lyra, V. A. Malyshev, and F. Dominguez-Adame, Phys. Lett. A **372**, 6694 (2008).
[13] A. Sacchetti, J. Phys. A: Math. Theor. **41**, 265304 (2008).
[14] C. Janot, L. Loreto, and R. Farinato, Phys. Lett. A **276**, 291 (2000).
[15] A. Buchleitner and A. R. Kolovsky, Phys. Rev. Lett. **91**, 253002 (2003); A. R. Kolovsky, Phys. Rev. A **70**, 015604 (2004).
[16] T. Schulte, S. Drenkelforth, G. K. Büning, W. Ertmer, J. Arlt, M. Lewenstein, and L. Santos, Phys. Rev. A **77**, 023610 (2008).
[17] T. Hartmann, F. Keck, H. J. Korsch, and S. Mossmann, New J. Phys. **6**, 2 (2004).
[18] This property follows readily from the relation $S(\kappa) \sim \Sigma_n c_n \exp(-in\kappa a)$ between Bloch (S) and Wannier (c_n) amplitudes of the state vector Ψ. The condition $\Sigma_n |c_n|^2 < \infty$ ensures the convergence of the series defining $S(\kappa)$ in the entire Brillouin zone.
[19] See, for instance, S. Longhi, Laser Photonics Rev. **3**, 243 (2009), and references therein.
[20] A. Szameit, F. Dreisow, T. Pertsch, S. Nolte, and A. Tünnermann, Opt. Express **15**, 1579 (2007).
[21] G. Lenz, I. Talanina, and C. M. de Sterke, Phys. Rev. Lett. **83**, 963 (1999).
[22] N. K. Efremidis and D. N. Christodoulides, Phys. Rev. E **65**, 056607 (2002).
[23] As the chain is terminated at $n=N=73$, to avoid reflections due to array truncation, smoothly absorbing boundary conditions have been assumed on the right-hand side of the integration domain.